Published in final edited form as:
Immunity. 2008 November ; 29(5): 807–818. doi:10.1016/j.immuni.2008.09.013.

Receptor-independent, direct membrane binding leads to cell surface lipid sorting and Syk kinase activation in dendritic cells

Gilbert Ng[1,*], **Karan Sharma**[1,*], **Sandra M. Ward**[2], **Melanie D. Desrosiers**[1], **Leslie A. Stephens**[1], **W. Michael Schoel**[3], **Tonglei Li**[4], **Clifford A. Lowell**[5], **Chang-Chun Ling**[2], **Matthias W. Amrein**[3], and **Yan Shi**[1]

1*Immunology Research Group, Department of Microbiology and Infectious Diseases, University of Calgary, Calgary, Alberta T2N 4N1, Canada*

2*Department of Chemistry, University of Calgary, Calgary, Alberta T2N 4N1, Canada*

3*Department of Biology and Anatomy, University of Calgary, Calgary, Alberta T2N 4N1, Canada*

4*Department of Pharmaceutical Sciences, University of Kentucky, Lexington, Kentucky 40536, U.S.A.*

5*Department of Laboratory Medicine, University of California San Francisco, San Francisco, California 94143, U.S.A.*

Summary

Binding of particulate antigens by antigen presenting cells (APC) is a critical step in immune activation. Previously, we demonstrated that uric acid crystals are potent adjuvants, initiating a robust adaptive immune response. However, the mechanisms of activation are unknown. Using atomic force microscopy as a tool for real time single cell activation analysis, we report that uric acid crystals can directly engage cellular membranes, particularly the cholesterol components, with a force substantially stronger than protein based cellular contacts. Binding of particulate substances activates Syk kinase-dependent signaling in dendritic cells (DCs). These observations suggest a mechanism whereby immune cell activation can be triggered by solid structures via membrane lipid alteration without the requirement for specific cell surface receptors, and a testable hypothesis for crystal-associated arthropathies, inflammation and adjuvanticity.

Introduction

Receptor and ligand interactions are the pillar of modern biomedical research. They permeate vast categories of cellular activities. The tenet of receptor activation is the specificity. Antigen presenting cells (APCs) are the sentinels of the immune system. They detect signals of infection and tissue stress. Some well-studied triggers of APCs are PAMPs (Pathogen-associated molecular patterns), first suggested by Charles Janeway in the late 80s' and subsequently verified experimentally (Janeway, 1989). These substances, such as lipopolysaccharides, double-stranded RNA, etc., are only produced by microbes and trigger a set of conserved receptors (Toll-like Receptors, TLRs) on mammalian host cells. Upon detecting these

Correspondence: Yan Shi, B872 HSC, 3330 Hospital Dr. NW, University of Calgary, Calgary, Alberta, Canada, Phone 403-220-2536, Fax 403-270-2772, email: yshi@ucalgary.ca.
*These two authors contributed equally to this work

substances, APCs are activated with a very well-characterized signaling cascade involving adaptor molecules Myd88, Trif, and others, and eventually leading to nuclear translocation of NFκb (Fitzgerald and Chen, 2006; Takeda et al., 2003).

APCs, particularly dendritic cells (DCs), are also triggered by environmental factors, such as physical disturbance and the presence of particulate structures. The related activation mechanisms are largely unknown. For example, we identified several years ago that monosodium urate (MSU) crystals, as an endogenous stress signal, strongly activate DCs (Shi et al., 2003). Several reports have since implicated its involvement in various aspects of the immune system, including inflammation (Chen et al., 2006), tumor immunity (Hu et al., 2004), autoimmune diabetes (Shi et al., 2006) and antibody response (Behrens et al., 2008). There have also been studies on the mechanisms of MSU-mediated cellular activation. IL-1β (Chen et al., 2006) and Nalp3 inflammasome (Martinon et al., 2006) are reportedly involved. Historically, MSU has been known to induce robust inflammation from epithelial and monocytic cells, and are the causative agent of gout (Smyth and Holers, 1998). Despite its biological relevance, how MSU crystals interact with our tissues, particularly the initial contact with APCs, remains unknown. It has been suggested that certain structures related to the TLR/PAMPs might contribute to the biological activities (Liu-Bryan et al., 2005; Scott et al., 2006). However, the fact remains that MSU crystals trigger APCs even under Myd88/Trif double deficiency and none of the TLR knockouts showed reduced response to MSU (Chen et al., 2006) (and see the results), ultimately ruling out any similarities with the canonical TLR signaling mechanisms. Being a continuous crystalline surface, it is difficult to imagine any protein-based receptor that would specifically recognize the structure, and our attempts to isolate such receptors have not been successful. It stands to reason that being nearly omni-responsive, even to post-industrial materials, there will be no evolutionarily co-developed receptors on APCs that can see everything. Therefore, conventional receptor ligand interactions might not explain this category of events. This is a clear caveat of the PAMP/TLR paradigm. Many years ago, it was proposed that a crystal's surface electrostatic state and its molecular "ruggedness" determined their potential to induce inflammation in host cells. In other words, it was attributed to a generic membrane activation event that led to subsequent cellular activities (Mandel, 1994; Mandel, 1976). This line of research has diminished under the elegance of receptor-based activation. We, however, decided to study whether non-receptor based modes of engagement of MSU could lead to DC activation.

In this report, we present an alternative hypothesis that membrane affinity for external objects might lead to plasma membrane lipid sorting. Specifically, using atomic force microscope as a tool for single cell affinity analysis, we present evidence that a solid surface may form electrostatic bonding with plasma membrane cholesterol. This bonding may lead to the aggregation of lipid rafts which in turn use their associated intracellular ITAMs to recruit Syk kinase, leading to PI3K activation and permitting subsequent DC activation. This hypothesis may explain why DCs respond to solid structures even without a clear receptor ligand interaction, and opens an intriguing new window into how crystals interact with tissues.

Results

1. MSU crystal mediated DC activation does not require Myd88/Trif

We previously reported that DC activation by MSU was independent of TLR4, and MSU crystals were not recognized by any known TLRs (Chen et al., 2006; Shi et al., 2003). To more thoroughly eliminate the involvement of PAMPs, we tested this activation in Myd88 (not shown) and Myd88 + Trif double knockout (DKO) DCs because they lack both arms of TLR mediated signaling. We found that CD86 upregulation was present (Fig. 1A), similar to wildtype DCs. In search of any potential mechanisms that do not require cell surface receptors, we first removed membrane cholesterol from cells with methyl-β cyclodextran (MBCD) and

blocked actin microfilament movement with cytochalasin B. Both treatments dramatically reduced DC activation following exposure to MSU crystals (Fig. 1B and C) while most PAMP-mediated activations were far less sensitive. This preliminary work implicates more forcefully the involvement of activation mechanisms other than PAMPs/TLRs, hinting at a role of cell membrane lipids and cellular morphology. We verified the result by testing DC-like THP-1 cells (induced by PMA) of their production of IL-1β in response to MSU crystals, which is a robust and well-documented standard assay. It is clear that MBCD and cytochalasin B blocked this activation as well (Fig. 1D).

2. MSU/DC interaction study with AFM based single cell analysis

To study cell surface engagement of MSU crystals, it was important to design a single cell-based analysis tool. Because large continuous crystalline surfaces are difficult to control in their contacts with DCs (much longer and narrower than a regular cell), we decided to use Atomic Force Microscopy (AFM) to study the detailed interactions between MSU and DC surface. Using laser forceps or the AFM itself and assisted by a microscope, MSU crystals were individually glued to the tip of an AFM cantilever (Fig. 2A upper left panel). The modified cantilever was lowered to make contact with an assortment of DCs grown on glass disk (Fig. 2A upper right panel). Specifically, the crystal-coated cantilever was continuously scanned towards and away from the cell over a range of five microns at 3 seconds per cycle. The cycling was initiated even before the microscope head was close enough to the sample to establish a contact. The microscope head was then gradually lowered to the surface in 0.5 to 2 um increments of vertical descent (Fig. 2A lower panels) until an intermitted contact between the crystal and the cell was established upon each cycle. We started to collect force curves at the first contact indicated by any force of adhesion. Each individual force curve was analyzed for its maximum adhesion force (i.e. the force needed to separate the crystal from the cell). This circular mode was chosen because longer, stationary contacts yielded binding forces beyond the optimal ranges of our current AFM setup. Moreover, measuring the adhesion force every three seconds allowed us to plot the binding strength over time. DCs produced increasing affinities measured by the AFM tip, from initial values between 50–200 pN (pico Newton) basal readings to the point of enormous strength where the plasma membrane was likely ruptured in some cases in the elevating phase of the tip (over 10 nN) (Fig. 2B). This interaction was seen with bone marrow-derived (BM) DCs and DC lines (DC2.4 and PMA induced THP-1) (Shen et al., 1997), but only in the presence of the MSU crystal as control blank cantilevers produced only basal affinities (Fig. 2C). The binding force was present with DCs from Myd88 +Trif DKO, but eliminated with cytochalasin B or MBCD treatment (Fig. 2D and E). These data suggest that the contact with the small crystal induced a cellular event that was defined by extremely strong affinities. This contact force appeared to be associated with DCs since control cell lines (NIH Balb/c 3T3, a fibroblast, and B16, a melanoma) did not sense the presence of the crystal and produced no increased force curve (Fig 2F).

3. MSU/DC interaction is of high affinity and does not require specific surface receptors

To our knowledge, force contacts generated during cellular interactions are in the range of pN (Panorchan et al., 2006a; Panorchan et al., 2006b). We are not aware of any report that described such a strong interaction. To compare this to a more defined immune activation, we stimulated T cell antigen receptor (TcR) transgenic T cells (OT-1 CD8+ T cells and OT-2 CD4+ T cells), and by using biocompatible glue Cell-Tak (Waite and Tanzer, 1981), attached individual T cells on to the tip of an AFM cantilever, and lowered the T cells to make contact with DCs (Fig. 3A). In the absence of peptide antigen, we observed forces in the range of low pN, whereas with peptides, (SIINFEKL and ISQAVHAAHAEINEAGR for OT-1 and OT-2, respectively), the forces went up 10-fold for both MHC class I (about 200 pN) and class II (about 100 pN)-mediated interactions (Fig 3B), but never reached the magnitude between the MSU crystal and the DCs (in nN range) (Fig. 2). This indicated that MSU and DC engagement was different

from a protein-based interaction. To this end, we removed cell surface proteins with pronase, which eliminated at least 90% of total surface proteins, as determined by the loss of biotin labeling (Fig. 3C). Treated DCs were no longer able to bind to a glass surface because that class of binding is protein dependent. To circumvent this difficulty, we stabilized treated cells with a nickel grid with pore size of 5 uM by gentle centrifugation, so that trapped cells were no longer able to move freely (Fig. 3C). When the MSU tip was lowered to the exposed part of the treated cells, the contact force was again reproduced (Fig. 3D). To determine whether what we observed was a specific event, we reversed that orientation of our setup and attached the DCs to the tip and lowered the tip to be in contact with an assortment of crystals and control surfaces (Fig. 3E). Because in this setup the contact surfaces were larger, the forces were accordingly stronger (Fig. 3E). We detected increased forces between the tip and MSU, and latex beads, two structures that are known to interact with DCs (Kovacsovics-Bankowski and Rock, 1995; Shi et al., 2003). Interestingly, control crystals, including basic calcium phosphate (BCP) and allopurinol, which we reported before to be unable to activate DCs, failed to produce the force curves by this assay as well (Fig. 3E) (Shi et al., 2003).

4. Syk recruitment to membrane associated ITAMs is required for MSU/DC binding

We were interested in the downstream intracellular events of this membrane protein-independent activation. We treated cells with Wortmannin and LY-294002, blockers of PI3 kinases (PI3K), and detected a complete abolishment of the interaction (Fig. 4A). In inflammatory phagocytosis, which we speculate is mechanistically related to our observations, PI3K activation results from the recruitment of Syk to the cell membrane. This recruitment is mediated by the interaction between receptor complexes bearing immunoreceptor tyrosine-based motifs (ITAMs), which are present in FcR̨γ and DAP12 adapter proteins in myeloid cells (Lanier et al., 1998), and the SH2 domains on Syk (Aderem and Underhill, 1999;Underhill and Ozinsky, 2002). Because Syk-deficient mice are non-viable, we first tested the effect of Piceatannol, a general blocker of Syk, and saw a complete blockage of affinity binding and cellular activation (Fig. 4A). A Syk inhibitor specificity control, ER 27319, which only blocks the interactions between Syk and the ITAM on FcR ε chain on mast cells but not other Syk/ITAM interactions (Moriya et al., 1997), did not alter the force curve (Fig. 4A). In these experiments, it is important to note that DCs removed of surface proteins are sensitive to Syk and PI3K inhibitions as well, suggesting that a signal is delivered across the membrane to these kinases without the presence of specific receptors (Fig 4B). We tested the MSU activation of DCs prepared from mice lacking either or both FcRγ/DAP12 (Humphrey et al., 2005). The forces curves were still detectable in most cases (Fig. 4C), suggesting that additional ITAM-containing proteins contribute to the Syk membrane recruitment. Further supporting our hypothesis, external blocking with an anti-FcR γ antibody (2.4G1) did not diminish the binding force (Fig. 4A). A role for Syk was confirmed by using DCs prepared from irradiation bone marrow chimeric mice reconstituted with fetal liver from $Syk^{-/-}$ C57BL/6 mice (Crowley et al., 1997). Activation by MSU was abrogated in the $Syk^{-/-}$ DC (Fig. 4D). Because basal phosphorylation of ITAMs requires upstream Src kinase activities, we also tested Hck/Fgr/Lyn triple knockout DCs (Src TKO) (Fitzer-Attas et al., 2000). We detected a delayed binding force (Fig. 4E) in some DC preparations while the other preparations of Src TKO DCs had very low binding (not shown). Similar to their role in other cell functions, such as FcR-mediated phagocytosis where Src family kinases are required for the Syk phosphorylation, Src TKO might not block all the related biological events, owing to other Src activities (Fitzer-Attas et al., 2000) (personal communication with L. Lanier). This notion was confirmed in our analysis with SU6656, a highly potent Src inhibitor. SU6656-treated DCs completely lost their interaction with MSU crystals (Fig. 4F) after 2 hour or longer incubation, presumably allowing ITAM phosphorylation turnover. Since Syk involvement in MSU mediated activation was new, we measured its phosphorylation status with intracellular staining. Clearly, phosphorylated Syk was detectable after the MSU engagement, and subsided in less than 60 minutes (Fig. 4G).

The requirement for Syk and Src family kinases for MSU crystal stimulation were also observed in assays measuring upregulation of CD86 (Fig. 4H), suggesting the binding forces be an indicator of DC activation, or at least function in parallel to the latter event. We certainly do not know if there are any mechanistic connections between the two sets of events. We postulate that in Src TKO, the basal ITAM phosphorylation is weaker and influenced by variations in DC preparations that led to the somewhat variable readings of Figure 4E.

In addition, to ascertain that such a binding event is not unique to MSU crystals, we glued latex beads to the AFM tip because of their strong affinity shown in Figure 3E, and detected a parallel sensitivity to cholesterol, actin, Syk and Src kinase blockage (Fig. 4I). This result suggests that such a receptor independent binding event is possibly applicable for other solid structure phagocytosis, although this point has not been experimentally substantiated.

5. MSU aggregates DC membrane cholesterol

Without surface protein receptors, we hypothesize that MSU surface binds to certain membrane lipid moieties and triggers a series of progressive membrane events. The most critical question remains which surface moiety is mediating such a contact, and how Syk is activated in response to this interaction. We loaded DCs with multiple fluorescence lipid probes and used a confocal fluorescence microscopy to capture the lipid distribution on the cell surface. While distribution and intensity of various labels may not be exactly similar, it is still noteworthy that phosphatidylcholine (PC) and phosphatidylethanolamine (PE) did not show any redistribution upon crystal binding, cholesterol showed a visible accumulation at the points of crystal contact (Fig. 5A), although not all sites of contact demonstrated this enhanced fluorescence, possibly suggesting that the membrane lipid ligation is a transient event, or that most functional cholesterol (lipid rafts) aggregates are under the limit of optical diffraction. The finding is nevertheless in line with our earlier observation that MBCD inhibited DC activation and their force curves. It is important to note that LPS treated DCs do not show the cholesterol redistribution characteristic of MSU binding (Fig. 5A). To ascertain that the distribution of cholesterol is indeed caused by MSU binding, we decided to study both light field and UV field for the location of cell and crystal. It should be noted that most MSU crystals bound to the DC surface and cause cholesterol sorting are no longer visible in the bright field. To circumvent the problem, we selected a rare case where a larger crystal was in contact with a cell. Although such an encounter is not representative, it does show that cholesterol undergoes substantial redistribution upon the binding of this crystal (Fig. 5A). We then tested monomeric fluorescence lipids for their binding to MSU crystal surfaces, and saw a stronger binding of cholesterol than other control lipids, PE and PC, despite their similar emission intensities (Fig. 5B). This testing method is only suggestive, as lipids do not interact with crystals in this manner. To definitively prove that the interaction between cholesterol and MSU is of high affinity, we produced an artificial outer plasma membrane leaflet with pure phosphatidylcholine (PC), as well as mixtures of PC/cholesterol and PC/sphingomyelin. The synthetic membranes were laid on a freshly cleaved mica surface and a MSU AFM tip was lowered to produce contact. It was clear that the monolayer containing cholesterol produced higher binding forces (Fig. 5C).

6. Synthetic cholesterol in its physiologic orientation shows direct binding to MSU

To more precisely define the role of cholesterol, we chemically attached a hydrocarbon chain ending with a thiol group to the cholesterol hydroxyl group (Fig. 6A). This thiol group was then attached to a gold-coated AFM cantilever by the self-assembly membrane. We then lowered the tip to a surface coated with MSU crystals. This procedure produces an “upside down” configuration in reference to cholesterol’s natural orientation in the plasma membrane, and accordingly produced binding forces very close to zero (Fig. 6B). To produce cholesterol in the correct orientation, the thiol group was to be attached from the other side of the molecule. Since it is chemically infeasible to directly modify cholesterol in this manner, a second analog

was prepared starting from cholic acid which contains a carboxylic acid group. A hydrophobic chain terminated with a thiol group was attached to the carboxylic acid group (Fig. 6A). The positioning of the alphatic chain at the other end of the cholesterol skeleton allowed us to produce a cholesterol configuration mimicking its natural orientation. When this synthetic cholesterol analog was attached to the cantilever, it produced significantly higher binding forces with MSU coated glass surface (Fig. 6B), suggesting that cholesterol in its biological configuration may interact with MSU crystals.

Discussion

Our work suggests that at least for DCs, surface contact is sufficient to introduce an activation signal across the plasma membrane, leading to an intracellular signaling cascade that involves Syk. It is well established that lipid raft aggregation significantly facilitates many signaling events. In IgE-mediated mast cell activation, one theory states that the function of surface receptors is to bring together sufficient amounts of lipid rafts of which cholesterol is an important component (Brown, 2006; Brown and London, 1998). The function of different membrane lipids in segregating surface proteins is well-known (Zacharias et al., 2002). ITAM-containing receptors are attracted to cholesterol rich regions on the cell surface. However, because lipid rafts prior to receptor ligation are small (less than 60 nM in diameter), random accumulation of receptors with activating motifs such as ITAM at any given point is low, balanced by efficient dispersion (Kusumi et al., 2004). If cholesterol is stabilized, the aggregation of lipid rafts may by themselves allow certain membrane events to take place, leading to cellular activation. Evidence supporting this mechanism comes from the assay where GM1, another component of lipid rafts, was crosslinked. The crosslinking induced significant membrane reorganization (Dietrich et al., 2001). This process is clearly not activated by protein receptor interaction. Syk membrane recruitment is triggered by protein receptor ligation that leads to phosphorylation of ITAMs, such as those present in BCR and FcR (Abram and Lowell, 2007). However, basal level ITAM phosphorylation is commonly observed. Since MSU engages a large continuous membrane surface, it may trigger sufficient recruitment of Syk to the inner leaflet (Fig 7). This hypothesis also explains why control cell lines do not interact strongly with MSU crystal as Syk is a hematopoietic kinase. Approaching the issue from a different angle, in several separate studies, it has been reported that membrane sorting occurs under the influence of membrane curvature and force (van Meer and Vaz, 2005), leading to highly concentrated lipid species confined in a space, such as an elongated tube, as a consequence. Reasoning from this prospective, the binding of any particular lipid moiety may not be crucial, as long as an external object has affinity to the plasma membrane. Because such an affinity based contact inevitably leads to membrane curvature. We noted with interest that in a most recent paper, it was shown that Shiga toxin may bind to surface structure, which leads to invagination and endocytosis as a pure lipid membrane event (Romer et al., 2007). Under our experimental settings, we have collected some evidence to suggest that MSU may interact with cholesterol. Whether it occurs under any biological conditions, and if so whether it has any biological meanings remains to be ascertained. However, even if another membrane moiety plays some or a large part of crystal binding, our proposal of force-induced lipid sorting may still stand. As one of our many possibilities, we would like to suggest on theoretical grounds that MSU crystal surface with a collective zeta potential of −37.4 mV (data not shown) might allow hydrogen bonding with properly packed cholesterol following lipid sorting. This suggestion is certainly speculative and solid surface chemistry work is needed to delineate the interaction.

Regarding the possibility of cholesterol sorting mediated by the crystal, some theoretical considerations may suggest that such an interaction could take place, unlike other H-bond forming partners. One feature of membrane lipids is their propensity to produce dense molecular “packing” into a structure that could even be aligned with the lattice of the crystal.

This would allow for a large number of H-bonds to occur per given surface area explaining the strong adhesive interaction. H-bonds formed with protein molecules are by comparison dispersed, because individual polypeptide chains cannot be sorted to such a density. Another detail that may facilitate this steady interaction is the ability of cholesterol to increase the bending rigidity of bilayer membranes and thus strongly suppresses their thermal undulations (manuscript in preparation). This in turn significantly reduces the entropic repulsion between the approaching surfaces. How these factors are incorporated into our specific case will be a topic of study for years to come.

We propose a two step, receptor-independent APC activation mechanism as follows: 1. MSU forms a spatially tight inter-molecular bonding (possibly hydrogen bond) with cholesterol within the first 30 seconds or less and the binding leads to lipid sorting due to the fluidity of the membrane. The force at this stage by our measurement is no more than 200 pN. 2. Lipid sorting aggregates ITAM-containing receptors which are preferentially segregated into cholesterol/sphingolipid rich regions of lipid rafts. It should be noted that ITAM-containing receptors are common in immune cells. 3. On DCs, Syk kinase is recruited by this accumulation and subsequently turns on PI3K. Syk is a hematopoietic kinase, and its functional association with downstream PI3Ks is unique in DCs or other phagocytes (Greenberg and Grinstein, 2002), and 4. This activation may trigger activities mediated by PI3Ks that is tightly linked to actin/microfilament movement, and the structural alterations brought about by the cytochalasin sensitive entities lead to auto amplification, permitting further accumulation of signaling molecules at the plasma membrane with higher degrees of phosphorylation, and larger contacts to be formed with the crystal. The force at this stage is in the nN range. Since these two steps are experimentally continuous, they manifest as a two phased force curve change. It is important to note that while Syk and PI3K are required for the binding, it was interesting the ITAM DKO and Src TKO DCs retained the affinity, although in some cases they were lower than WT DCs. We would like to suggest that additional ITAM-containing membrane structures, such as GVPI and WSL-1 (Gardiner et al., 2008; Lohi and Lehto, 1998) and Src kinases, such as Src itself and Abi and Csk provided the residual functionality (Hughes, 1996).

It is worth further emphasizing that the central hypothesis of our work is the ability of sorted lipid domains to attract ample signaling molecules to a highly localized area on the cell surface. The ITAM containing adaptor molecules, often associated with lipid rafts, are an important intermediate although their identities may not be crucial. They serve to nonspecifically attract Syk kinases to the surface as they do in the receptor-based Syk recruitment. How the specific activation events mediated by this generic kinase recruitment differ from other receptor mediated counterparts need to be analyzed in greater details in the future. From our work, it appears that an event akin to phagocytosis does take place.

An important question yet to be addressed is how "complete" the signaling cascade is in such a lipid based interaction, in terms of common markers of DC activation (CD86, cytokine and phagocytic capacities etc). The pronase treatment is harsh and cells die within 2 hours and before any subsequent activation events can be measured. Any evidence deduced from assays without complete removal of surface proteins should be viewed with suspicion of residual receptor based activities. This report therefore, is incomplete in this regard due to the limits of our technologies as far as blocking all protein based interactions without affecting overall state of cellular viability. Syk mediated PI3K activities are well documented (Aderem and Underhill, 1999; Greenberg and Grinstein, 2002; Underhill and Ozinsky, 2002). However, MSU mediated "complete" DC activation requires Nalp3 inflammasomes (Martinon et al., 2006). Information directly linking these two categories of signaling events is yet scarce and suggestive. For instance MAPK activation is triggered by Syk (Wan et al., 1996) which in turn may be linked to inflammasomes and other cellular activations (Shaw et al., 2008). In our view, our study illustrates the link between surface lipid sorting and Syk kinase activation. Since the Syk/PI3K

pathway is suggested to be inflammatory such as in the case of FcR gamma mediated phagocytosis, MSU mediated lipid sorting by inference may be linked to "inflammatory phagocytosis". Associations with other downstream events are a matter of speculation, and they only serve as "readouts" for this study. It is entirely possible that Nalp3 mediated DC activation depends on some protein-based recognition of the crystal surface, and the lipid binding merely serves as a pre-requisite for other events to take place.

This report provides an explanation of how particulate materials, even without any known mechanism, may trigger strong DC activation, in cases independent of opsonization and antibody binding (Fig 7). Broadly speaking, there is no reason to rule out this class of cellular interaction in other signaling settings, including those with receptors, as ligation forces/membrane contact are integral parts of signal exchange. It was a surprise finding that DCs showed ever-increasing affinity to a solid structure without its surface proteins (Fig 3D). Being adoptive to the enormous variances of binding targets and being independent of the surface proteins, our results seem to imply that outer membrane undergoes some form of lipid sorting/reconfiguration to maximize the binding affinity following each contact, although this suggestion needs intense scrutiny. How membrane lipids engage diverse solid surfaces with increasing binding strength as a consequence of intracellular signaling is puzzling and will be a topic of future studies.

Our work has several implications. First, crystal-induced diseases, such as gout and calcium salt deposition, are historic topics of medicine that so far have not been explained at molecular levels. Our work provides a testable hypothesis for that line of research. Second, phagocytosis has long been regarded as a receptor-based event (Stuart and Ezekowitz, 2008). That reasoning at times falls short in explaining why nearly all particulate substances including man-made synthetic materials, once entering tissues, trigger strong innate recognition. Our work puts this important topic under new light. Lastly, it should be pointed out that some of the best known adjuvants are crystals. Alum, the only FDA approved human vaccine enhancer, is a mixture of aluminum salt crystals. Despite its extensive usage in human and significant research on its cellular modulation (Jordan et al., 2004), we still do not have any understanding on its facilitating effect on antigen uptake. Membrane lipid interaction is a clear candidate for its mechanism. Overall, our work suggests that innate recognition has an extension unrelated to TLR/PAMPs.

Beyond proposing a new mechanism for Syk mediated DC activation, several lines of techniques employed in this work will likely have value for research in immunology. AFM based force measurements (cell hesion) are a valid alternative to conventional imaging analysis and other readings of cellular activation, as they obtain quantitative binding affinities in real time and the contacts are reversible on the fly, unlike stationary readings of imaging methods. They also have the advantage of efficiency as optimized experiments can be carried out in hours or minutes rather than days, and in theory, with one cell. The nickel mesh based trapping enables readings for non-adherent cells, which to our knowledge, has never been attempted before. We therefore believe these biophysical approaches will add functional tools for immunologic research and beyond.

Experimental Procedures

Mice, cells and reagents

All mouse strains were housed at University of Calgary Animal Research Centre (C57BL/6, OT-1, OT-2, Myd88 + Trif DKO) or University of California San Francisco animal facilities (FcR γ KO, DAP12 KO, FcR γ + DAP12 DKO, Hck +Fgr + Lyn triple KO, and Syk KO -> B6 fetal liver chimera). Some FcR γ KO mice were purchased from Jackson laboratories. Syk KO -> B6 BM DCs are microscopically indistinguishable from other DCs. Myd88 + Trif KO

mice were gifts from Dr. Paul Kubes (University of Calgary) and Dr. LianJun Shen (University of Massachusetts Medical School). Dendritic cell cultures, cell lines, cytokine kits, antibodies, flow cytometric analysis, and most reagents used in this work have been described previously (Desrosiers et al., 2007). Total Syk and Phos Syk antibodies were purchased from Santa Cruz and BD respectively and were used as instructed. Cytochalasin B, MBCD, LY-294002, Piceatannol, and PMA were purchased from Sigma. Wortmannin was from A.G. Scientific; SU6656 Calbiochem; and ER 27319 Tocris. THP-1 cells and DC2.4 cells were gifts from Dr. Peter Cresswell of Yale University and Dr. Kenneth Rock of University of Massachusetts Medical School, respectively. For THP-1 cytokine production, cells were plated at 2.5×10^5 cell per well in 12 well plate with 10 ng/ml PMA for 48 hours. Cells were then washed and treated with 5 ug/ml CpG or 100 ug/ml MSU for 24 hrs before ELISA analysis. All lipid probes were purchased from Molecular Probes (Invitrogen) and Avanti Lipids. SIINFEKL peptide was a gift from Dr. Kenneth Rock of University of Massachusetts Medical School, and ISQAVHAAHAEINEAGR was purchased from Cedar Lane.

Atomic Force Microscopy

The AFM work was performed on a Zeiss Axiovert 200 microscope under a JPK NanoWizard II AFM. Blank tipless cantilevers were purchased from Novascan and MikroMasch. MSU and control crystals (BCP and allopurinol) were produced as previously described (Shi et al., 2003). The crystal modified cantilevers (Novascan NPOWS 0.06 n/m) were custom made by Novascan assisted by a pair of laser tweezers for crystal selection and adhesion. They were also produced in house (University of Calgary) by adding freshly mixed epoxy resin and catalyst (Epoxy, etc. 10-3004C) to the tip of the cantilever under AFM control and subsequently moved to be on top of a MSU crystal of proper size for the adhesion after the contact. The modified cantilevers were heated on a hot plate to stabilize the glue. Latex tips (4.5 um) were produced similarly.

A similar modification process was used to glue individual DC2.4 cells to a Novascan NSC12 (0.06/m) cantilever. Glass disks coated with various crystals were produced as follows: allopurinol and basic calcium phosphate (BCP) crystal surfaces were produced by drying preformed crystal to glass disks which provide sufficient binding strength for AFM reading. MSU crystal surface was produced by first coating the disk with MSU crystal specific IgM antibody E6C7, and then the preformed MSU was allowed to bind to the underlying antibody. The production and biological relevance of MSU-specific IgM antibodies will be described in a separate manuscript (in preparation). Details of AFM operation are depicted in the supplemental data.

Blocking reagents, CD16/CD32 FcR blocker 2.4G1 (Ebioscience, clone 93), Wortmannin (A.G. Scientific W1022, 60 nM), cytochalasin B (Sigma 30380, 5 ug/ml), LY-294002 (Sigma L9908, 50 uM), Piceatannol (Sigma P0453, 50 uM), and ER 27319 (Tocris 2471, 30 uM) were added 30 minutes to 1 hour before the readings were taken. SU6656 (Calbiochem 572635, 10 nM) was added 2 hr or over night before the reading to allow the turnover of basal ITAM phosphorylation. For MBCD treatment for the AFM purpose, cells were washed twice with 10 mM of MBCD in cell culture media prior to the reading. The cells remained attached to the glass after this treatment.

The number of repeats of AFM force curve readings are indicated in the parenthesis in the figure legend. The ones without numbers are the basic readings, such as between MSU and DC2.4. All those curves were obtained more than 50 times for each interaction.

Affinity Force Reading between T cell and DC, and between tip bound and crystal surfaces

Eight million OT-1 and OT-2 splenocytes in 4 ml of culture media were stimulated with 10^{-10} M SIINFEKL peptide for one day and 200 ug/ml ovalbumin for 3 days, respectively. T cell blasts were laid on a glass disk under the AFM. A Novascan cantilever (NPOWS, 0.06 n/m) was first to make contact with a Cell-Tak (BD) droplet and then with the T cell. The cell-attached cantilever was immediately moved to another disk cover with DC2.4 cells and a procedure identical to the crystal and DC contact was performed. In some assays, 10^{-8} M SIINFEKL and 10^{-6} M ISQAVHAAHAEINEAGR were added to the DC disks prior to their contact with OT-1 and OT-2 cells, respectively, to measure force curves in the presence of antigens.

Surface protein removal and nickel grid cell trapping

Biotin (Sulfo-NHS) was purchased from Pierce. DC2.4 or THP-1 cells were labeled either in the plate directly or first removed by light trypsin treatment (which showed a much reduced biotin labeling). 0.5 mg/ml biotin in PBS was used to label cells at 37°C for 45 min. Cells were then washed and treated with 1 mg/ml pronase for 25–45 minutes either at RT or 37°C. The cells were then washed and stained with FITC-conjugated streptavidin for flow cytometric analysis. Some cells were lightly spun at 1000 rpm (Beckman Allegra X-15, SX4750 rotor, pre-warmed to 37°C) for 5 min onto a Tecan nickel mesh (8 um thick, with 5 um square holes) for the EM, and trapped cell binding force analysis. Under the AFM light microscope, the holes with cells trapped were identified by their partial blocking of AFM light source underneath. The tip of the cantilever was then moved to cover the remaining light as a guide for cell contact (the optical field is dark with nickel mesh except for the holes).

Producing cholesterol-coated AFM tips

On silicon probes with overall conductive Cr-Au coating from MikroMasch CSC38/Cr-Au (Wilsonville, OR), thiolated cholesterol analogs were allowed to form a self-assembled monolayer. The probes were immersed in 1 mM thiolated cholesterol in ethanol at 37°C for 5 days. The probes were then removed from ethanol prior to use.

Details of chemical syntheses of cholesterol and cholic acid derivatives, critical point dry, EM imaging and artificial membrane synthesis, as well as lipid/crystal binding and flow cytometry are provided as supplemental data.

Supplementary Material

Refer to Web version on PubMed Central for supplementary material.

Acknowledgements

We thank Dr. Lewis L. Lanier for his intellectual input, mice, review and editing of this manuscript. We thank Drs. Elmar Prenner, Kenneth Rock, LianJun Shen, Peter Cresswell, Paul Kubes, Pere Santamaria and Julie Deans for reagents and equipment. We thank Drs. Svetlana Baoukina, Kamala Patel, and Yang Yang for review and discussion. We thank Lynn Smith, Yongmei Hu, Christin Hollis, Dean Brown, Betty Chan, Vivian Yip, Jeff Yeung, Andrew Wu, Cherryl Panorel, Yin Fong, Tracy Flach, Joseph Andrews and Donna Preston for technical assistance. We thank Tecan Co. for the donation of nickel grid. This work was supported by grants to Y.S. from Alberta Heritage Foundation for Medical Research, Canadian Institute of Health Research and National Institutes of Health.

References

Abram CL, Lowell CA. The expanding role for ITAM-based signaling pathways in immune cells. Sci STKE 2007:re2. [PubMed: 17356173]

Aderem A, Underhill DM. Mechanisms of phagocytosis in macrophages. Annu Rev Immunol 1999;17:593–623. [PubMed: 10358769]

Behrens MD, Wagner WM, Krco CJ, Erskine CL, Kalli KR, Krempski J, Gad EA, Disis ML, Knutson KL. The endogenous danger signal, crystalline uric acid, signals for enhanced antibody immunity. Blood 2008;111:1472–1479. [PubMed: 18029553]

Brown DA. Lipid rafts, detergent-resistant membranes, and raft targeting signals. Physiology (Bethesda) 2006;21:430–439. [PubMed: 17119156]

Brown DA, London E. Functions of lipid rafts in biological membranes. Annu Rev Cell Dev Biol 1998;14:111–136. [PubMed: 9891780]

Chen CJ, Shi Y, Hearn A, Fitzgerald K, Golenbock D, Reed G, Akira S, Rock KL. MyD88-dependent IL-1 receptor signaling is essential for gouty inflammation stimulated by monosodium urate crystals. J Clin Invest 2006;116:2262–2271. [PubMed: 16886064]

Crowley MT, Costello PS, Fitzer-Attas CJ, Turner M, Meng F, Lowell C, Tybulewicz VL, DeFranco AL. A critical role for Syk in signal transduction and phagocytosis mediated by Fcgamma receptors on macrophages. J Exp Med 1997;186:1027–1039. [PubMed: 9314552]

Desrosiers MD, Cembrola KM, Fakir MJ, Stephens LA, Jama FM, Shameli A, Mehal WZ, Santamaria P, Shi Y. Adenosine deamination sustains dendritic cell activation in inflammation. J Immunol 2007;179:1884–1892. [PubMed: 17641055]

Dietrich C, Volovyk ZN, Levi M, Thompson NL, Jacobson K. Partitioning of Thy-1, GM1, and cross-linked phospholipid analogs into lipid rafts reconstituted in supported model membrane monolayers. Proc Natl Acad Sci U S A 2001;98:10642–10647. [PubMed: 11535814]

Fitzer-Attas CJ, Lowry M, Crowley MT, Finn AJ, Meng F, DeFranco AL, Lowell CA. Fcgamma receptor-mediated phagocytosis in macrophages lacking the Src family tyrosine kinases Hck, Fgr, and Lyn. J Exp Med 2000;191:669–682. [PubMed: 10684859]

Fitzgerald KA, Chen ZJ. Sorting out Toll signals. Cell 2006;125:834–836. [PubMed: 16751092]

Gardiner EE, Karunakaran D, Arthur JF, Mu F-T, Powell MS, Baker RI, Hogarth PM, Kahn ML, Andrews RK, Berndt MC. Dual ITAM-mediated proteolytic pathways for irreversible inactivation of platelet receptors: de-ITAM-izing Fc{gamma}RIIa. Blood 2008;111:165–174. [PubMed: 17848620]

Greenberg S, Grinstein S. Phagocytosis and innate immunity. Curr Opin Immunol 2002;14:136–145. [PubMed: 11790544]

Hu DE, Moore AM, Thomsen LL, Brindle KM. Uric acid promotes tumor immune rejection. Cancer Res 2004;64:5059–5062. [PubMed: 15289304]

Hughes AL. Evolution of the src-related protein tyrosine kinases. J Mol Evol 1996;42:247–256. [PubMed: 8919876]

Humphrey MB, Lanier LL, Nakamura MC. Role of ITAM-containing adapter proteins and their receptors in the immune system and bone. Immunol Rev 2005;208:50–65. [PubMed: 16313340]

Janeway CA Jr. Approaching the asymptote? Evolution and revolution in immunology. Cold Spring Harb Symp Quant Biol 1989;54:1–13. [PubMed: 2700931]

Jordan MB, Mills DM, Kappler J, Marrack P, Cambier JC. Promotion of B cell immune responses via an alum-induced myeloid cell population. Science 2004;304:1808–1810. [PubMed: 15205534]

Kovacsovics-Bankowski M, Rock KL. A phagosome-to-cytosol pathway for exogenous antigens presented on MHC class I molecules. Science 1995;267:243–246. [PubMed: 7809629]

Kusumi A, Koyama-Honda I, Suzuki K. Molecular dynamics and interactions for creation of stimulation-induced stabilized rafts from small unstable steady-state rafts. Traffic 2004;5:213–230. [PubMed: 15030563]

Lanier LL, Corliss BC, Wu J, Leong C, Phillips JH. Immunoreceptor DAP12 bearing a tyrosine-based activation motif is involved in activating NK cells. Nature 1998;391:703–707. [PubMed: 9490415]

Liu-Bryan R, Pritzker K, Firestein GS, Terkeltaub R. TLR2 signaling in chondrocytes drives calcium pyrophosphate dihydrate and monosodium urate crystal-induced nitric oxide generation. J Immunol 2005;174:5016–5023. [PubMed: 15814732]

Lohi O, Lehto VP. ITAM motif in an apoptosis-receptor. Apoptosis 1998;3:335–336. [PubMed: 14646480]

Mandel N. Crystal-membrane interaction in kidney stone disease. J Am Soc Nephrol 1994;5:S37–S45. [PubMed: 7873743]

Mandel NS. The structural basis of crystal-induced membranolysis. Arthritis Rheum 1976;19:439–445. [PubMed: 181020]

Martinon F, Petrilli V, Mayor A, Tardivel A, Tschopp J. Gout-associated uric acid crystals activate the NALP3 inflammasome. Nature 2006;440:237–241. [PubMed: 16407889]

Moriya K, Rivera J, Odom S, Sakuma Y, Muramato K, Yoshiuchi T, Miyamoto M, Yamada K. ER-27319, an acridone-related compound, inhibits release of antigen-induced allergic mediators from mast cells by selective inhibition of fcepsilon receptor I-mediated activation of Syk. Proc Natl Acad Sci U S A 1997;94:12539–12544. [PubMed: 9356485]

Panorchan P, George JP, Wirtz D. Probing intercellular interactions between vascular endothelial cadherin pairs at single-molecule resolution and in living cells. J Mol Biol 2006a;358:665–674. [PubMed: 16540120]

Panorchan P, Thompson MS, Davis KJ, Tseng Y, Konstantopoulos K, Wirtz D. Single-molecule analysis of cadherin-mediated cell-cell adhesion. J Cell Sci 2006b;119:66–74. [PubMed: 16371651]

Romer W, Berland L, Chambon V, Gaus K, Windschiegl B, Tenza D, Aly MR, Fraisier V, Florent JC, Perrais D, et al. Shiga toxin induces tubular membrane invaginations for its uptake into cells. Nature 2007;450:670–675. [PubMed: 18046403]

Scott P, Ma H, Viriyakosol S, Terkeltaub R, Liu-Bryan R. Engagement of CD14 mediates the inflammatory potential of monosodium urate crystals. J Immunol 2006;177:6370–6378. [PubMed: 17056568]

Shaw MH, Reimer T, Kim YG, Nunez G. NOD-like receptors (NLRs): bona fide intracellular microbial sensors. Curr Opin Immunol. 2008

Shen Z, Reznikoff G, Dranoff G, Rock KL. Cloned dendritic cells can present exogenous antigens on both MHC class I and class II molecules. J Immunol 1997;158:2723–2730. [PubMed: 9058806]

Shi Y, Evans JE, Rock KL. Molecular identification of a danger signal that alerts the immune system to dying cells. Nature 2003;425:516–521. [PubMed: 14520412]

Shi Y, Galusha SA, Rock KL. Cutting edge: elimination of an endogenous adjuvant reduces the activation of CD8 T lymphocytes to transplanted cells and in an autoimmune diabetes model. J Immunol 2006;176:3905–3908. [PubMed: 16547223]

Smyth, CJ.; Holers, VM. Gout, Hyperuricemia, and Other Crystal-Associated Arthropathies. New York: Marcel Dekker; 1998.

Stuart LM, Ezekowitz RA. Phagocytosis and comparative innate immunity: learning on the fly. Nat Rev Immunol 2008;8:131–141. [PubMed: 18219310]

Takeda K, Kaisho T, Akira S. Toll-like receptors. Annual Review of Immunology 2003;21:335–376.

Underhill DM, Ozinsky A. Phagocytosis of microbes: complexity in action. Annu Rev Immunol 2002;20:825–852. [PubMed: 11861619]

van Meer G, Vaz WL. Membrane curvature sorts lipids. Stabilized lipid rafts in membrane transport. EMBO Rep 2005;6:418–419. [PubMed: 15864292]

Waite JH, Tanzer ML. Polyphenolic Substance of Mytilus edulis: Novel Adhesive Containing L-Dopa and Hydroxyproline. Science 1981;212:1038–1040. [PubMed: 17779975]

Wan Y, Kurosaki T, Huang XY. Tyrosine kinases in activation of the MAP kinase cascade by G-protein-coupled receptors. Nature 1996;380:541–544. [PubMed: 8606776]

Zacharias DA, Violin JD, Newton AC, Tsien RY. Partitioning of lipid-modified monomeric GFPs into membrane microdomains of live cells. Science 2002;296:913–916. [PubMed: 11988576]

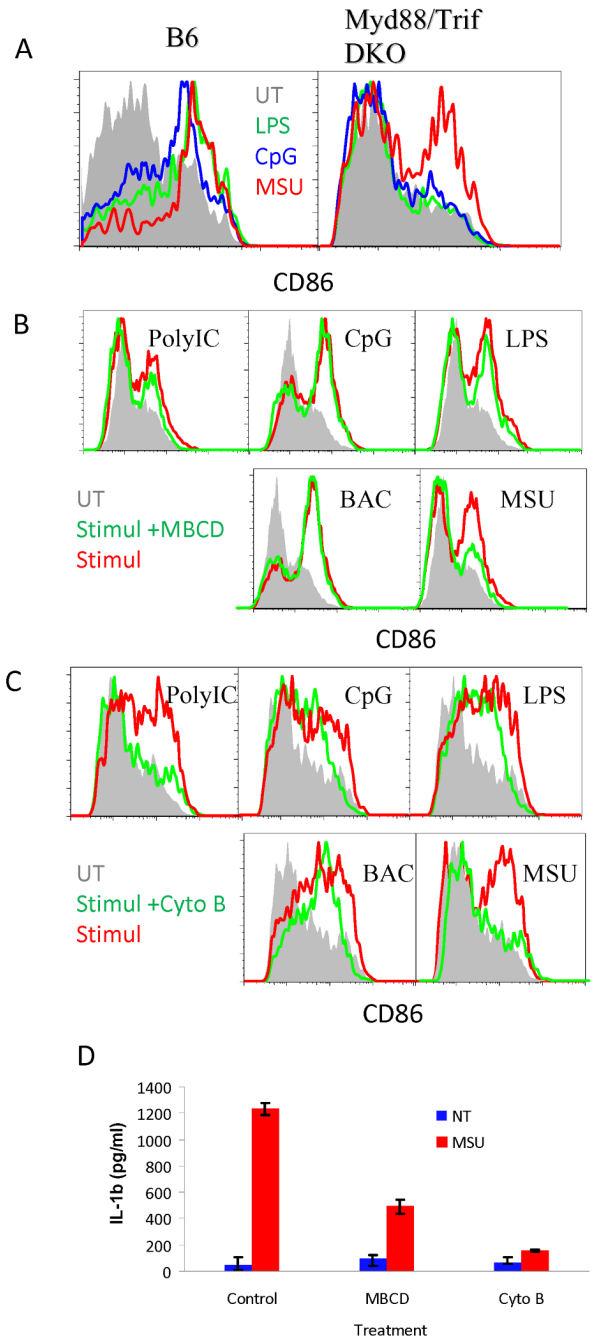

Fig 1. DC MSU crystal recognition depends on membrane cholesterol

A. BM DCs from C57BL/6 WT and Myd88 + TRIF DKO mice were grown as described, and stimulated with 10 ng/ml LPS, 5 ug/ml CpG, or 200 ug/ml MSU crystals for 5 hrs. CD86 expression on $CD11c^{+}$ cells was analyzed by flow cytometry. B. B6 BMDCs were extracted twice with 10 mM of MBCD in culture media (20 min each). Cells were treated as in A plus 100 ug/ml poly IC or 0.1 ul of killed *E. coli* (BAC) in 2 ml for 6 hrs in the presence of 2 mM MBCD to prevent membrane cholesterol restoration. Cells were analyzed as in A. C. Identical B except for cytochalasin B (1 ug/ml in the wells throughout the assay) was used in place of MBCD. D. THP-1 cells were stimulated as BM DCs for 6 hours and IL-1β production was measured by ELISA. The error bars represent 2 s.d..

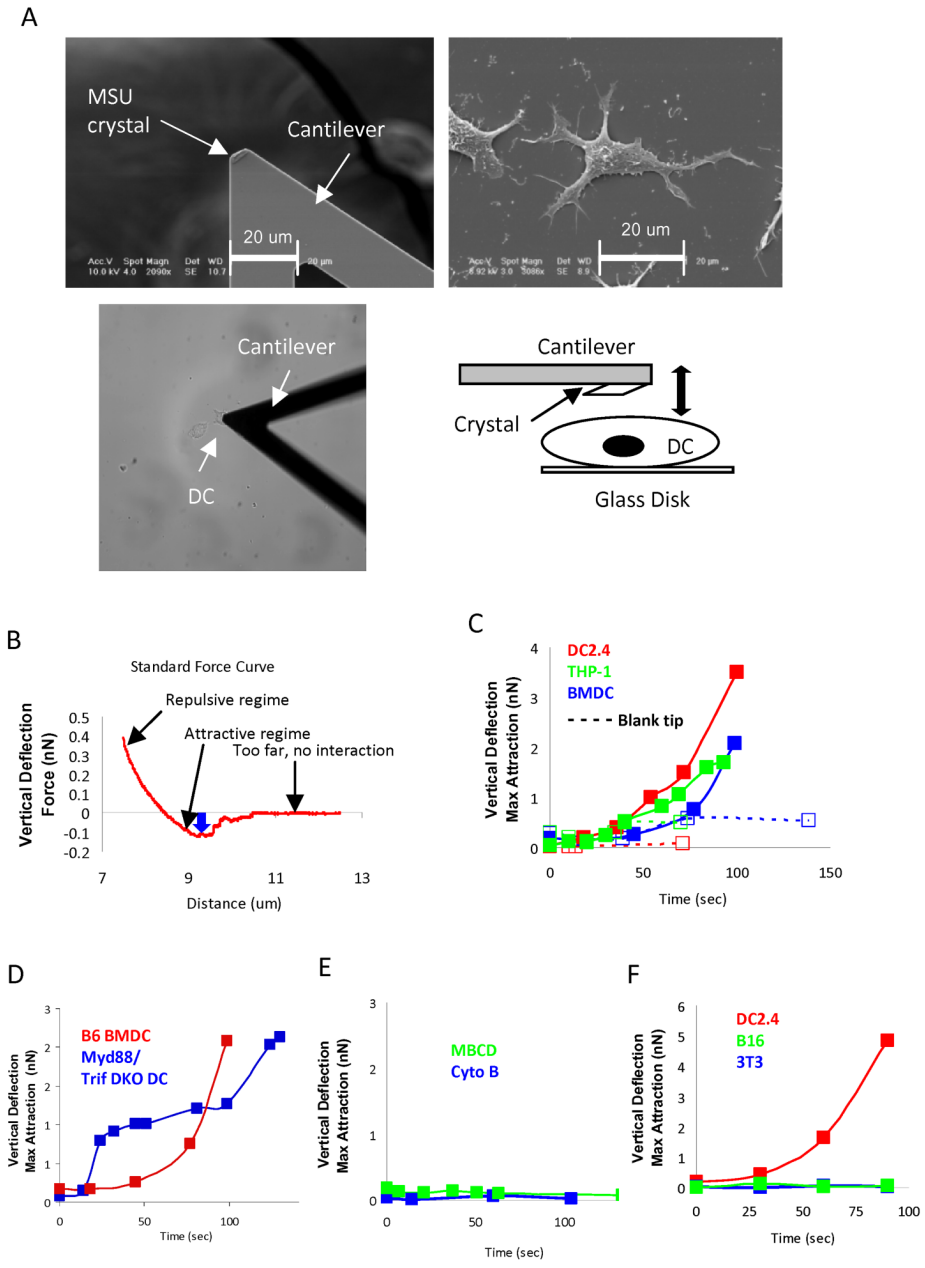

Fig 2. Binding of MSU crystal to DC membrane is of high affinity

A. Upper left: a SEM picture of a MSU crystal glued to the tip of an AFM cantilever; Upper right, a SEM picture of a DC2.4 cell that was cultured at low density; Lower left, a light camera picture of a MSU coated cantilever making contact with a DC, Lower right: a schematic abstract of cantilever with a MSU making contact with a DC. B. A sample force interaction generated by the technique illustrated in A. The distance measurement is at the center of the cell. The blue arrow indicates the maximum adhesion between crystal and the cell in pN or nN. The displacement indicated by the arrow was collected as one data point to plot the binding force change over time in the subsequent figures. Usually, 15 to 30 data points were collected for each binding force curve from which one maximal binding point was determined. C. Binding curves for DC2.4, THP-1, and B6 BM DCs with the MSU tip and a blank control tip (10, 8,

and 3). D. B6 BMDC binding force vs. Myd88+TRIF DKO DC (27). E. DC 2.4 binding curves in the presence of MBCD (4) or cytochalasin B (20), THP-1 and BM DCs produced identical data (not shown). F. Binding force of DC2.4 vs. two control non-hematopoietic cell lines, B16 (2) and NIH 3T3 (2).

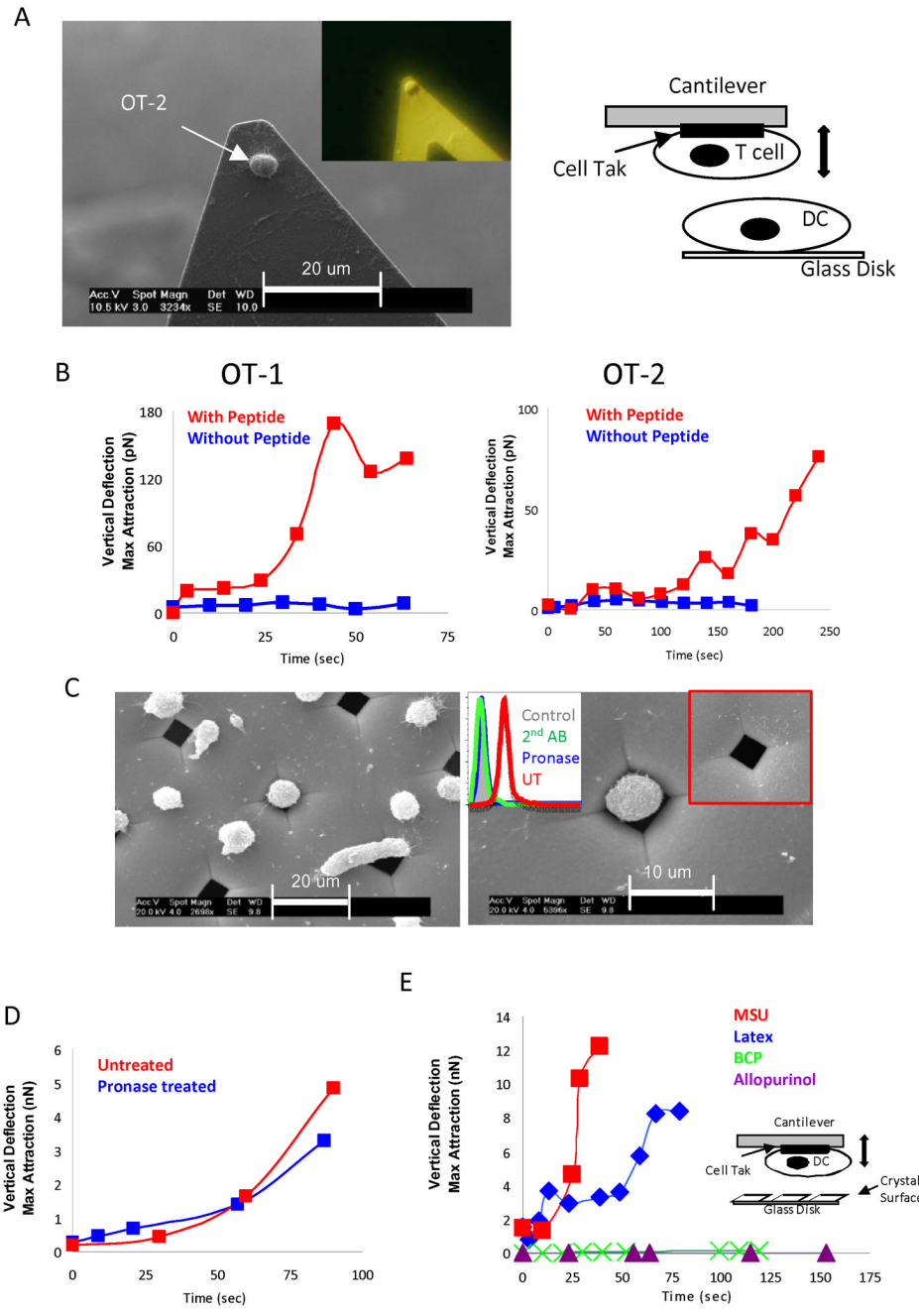

Fig 3. Binding of MSU to DCs does not require cell surface protein

A. Left: a SEM picture of an OT-2 cell glued to an AFM tip with Cell-Tak; insert: an image of a similarly glued OT-2 cell in pure alcohol without SEM processing, taken with a Nikon metallurgical white light epi-illumination microscope. Right: a schematic depiction of cantilever with a T cell making contact with a DC. B. Left, the binding force change of an OT-1 T cell glued to a cantilever to a DC2.4 with or without SIINFEKL peptide (7 and 6); right, the same set up except that an OT-2 T cell and ISQAVHAAHAEINEAGR peptide were used in place (7 and 4). C. Left. Pronase-treated DC2.4 cells were centrifuged to a nickel grid, and treated and analyzed similarly as in A. Right. A higher magnification of one cell trapped in the grid. The inserts are flow cytometric analysis of the biotin and FITC-conjugated streptavidin

staining of the DC2.4 cells with or without the pronase treatment, and an uncovered hole in the nickel mesh. D. The force curve of a DC2.4 cell trapped in the mesh after pronase treatment and its control (27). E. Force curves between a DC2.4 cell glued to a cantilever with the indicated crystal surfaces allopurinol (3), MSU (11) and BCP (3) or 1 um diameter latex beads attached (by heating/drying) to glass disks (7).

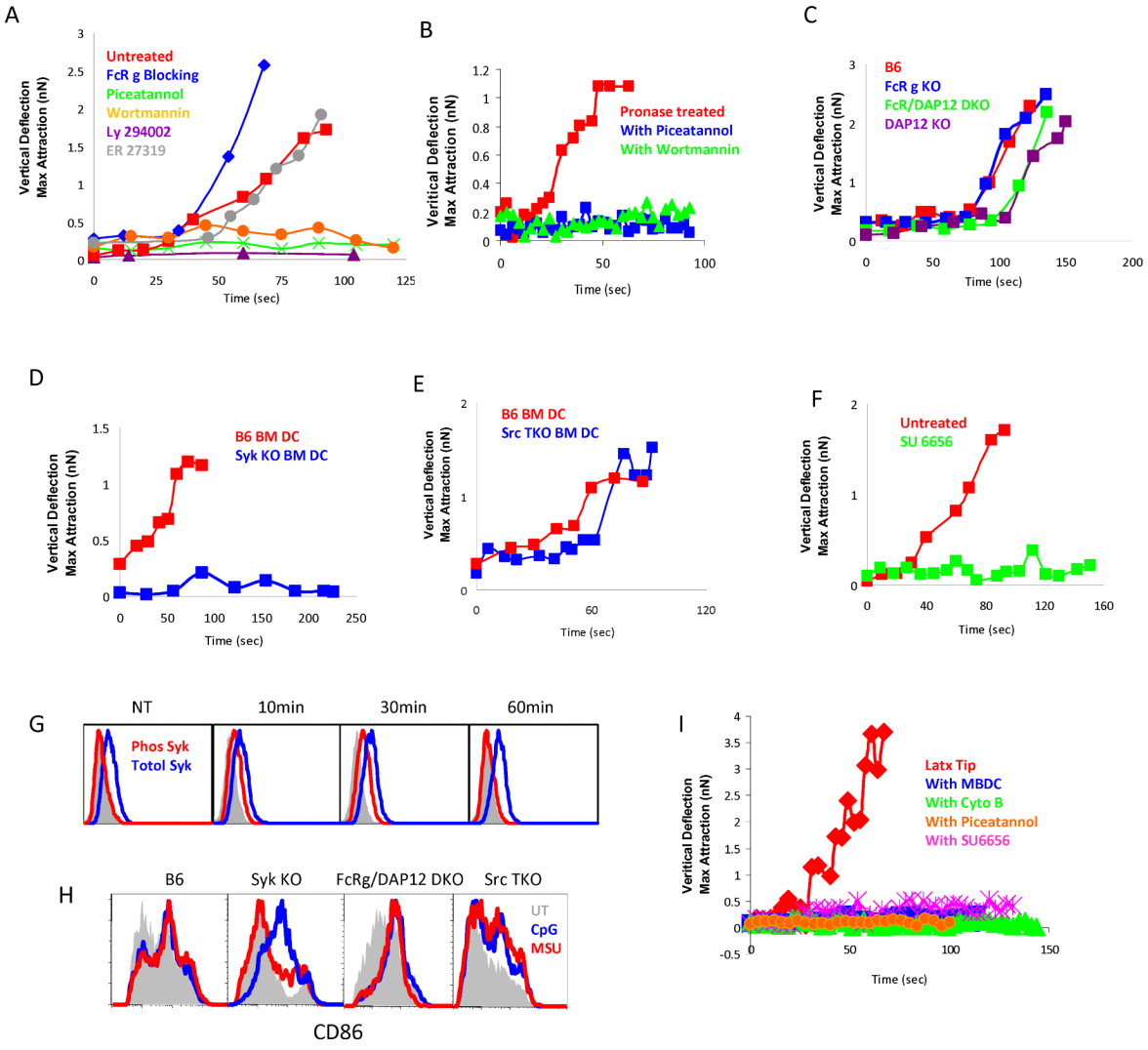

Fig 4. Syk kinase and basal ITAM phosphorylation are required for MSU binding and activation

A. As in Fig 2, force curves between DC2.4 and a MSU cantilever were analyzed in the presence of indicated Syk (Piceatannol 6 and ER27319 3), PI3K (Wortmannin 3 and Ly294002 6) or extracellular FcR γ blocker 2.4G1 (10). Similar data with other DCs are not shown. B. Similar to Fig. 3D for the pronase treatment. Cells were treated with either Syk (6) or PI3K inhibitor (6). C. Force curves between the MSU cantilever and the indicated BM DCs with ITAM-deficiencies: DAP12 KO (14), FcR γ KO (27) or DAP12 + FcR γ DKO (17). D. Force curves between MSU cantilever and BM DCs from Syk KO (21). E. Force curves between MSU cantilever and Hck + Fgr + Lyn triple Src KO BM DC (9). F. DC2.4 cell in the presence of the total Src activity blocker SU6656 (15). G. Phos Syk and total Syk were measured in permeabilized DC2.4 cells following MSU treatment as in Fig 1. H. Flow cytometric analysis of CD86 expression after MSU treatment as in Fig. 1 on BM DCs from the indicated KO or control mice. I. Similar to Fig. 4A except that latex tips were used in place of MSU tips, with or without (7) indicated MBCD (6), cyto B (10), SU6656 (7) or Piceatannol (5).

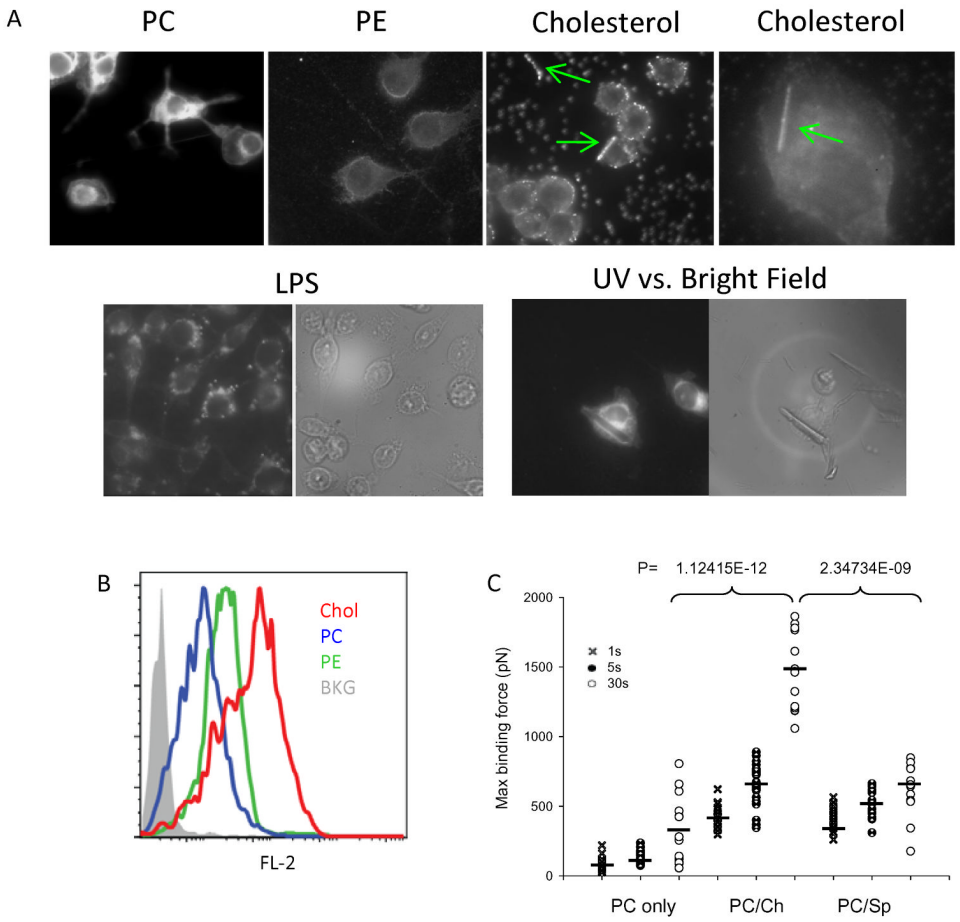

Fig 5. MSU crystals directly engage and sort membrane cholesterol

A. NBD (PC and PE) or Bodipy (cholesterol)-labeled lipids were used to label DC2.4 cells and MSU crystals were added to the labeled cells and analyzed under an AFM UV camera. Green arrows indicate the cholesterol sorting upon binding of MSU crystals. Cholesterol distribution on DC2.4 cells with LPS treatment were used as control. Also shown is a larger MSU crystal in contact with a DC2.4 cell to illustrate the cholesterol sorting underneath the crystal (most lipid sorting crystals are small and are only visible under UV when bound to cells). B. Equal amounts of labeled lipids (PE, PC or cholesterol) were used to stain MSU crystals and the stained crystals were analyzed by flow cytometry for the lipid binding. C. Synthetic bilayer plasma membrane with PC alone or with a mixture of PC/cholesterol or PC/sphingolipid was laid on freshly cleaved mica. A MSU cantilever was used to measure the binding forces after a hold of 1, 5, or 30 sec. P values were calculated by the t-test on maximum attraction forces. The black bar among the symbols is the average value for that group.

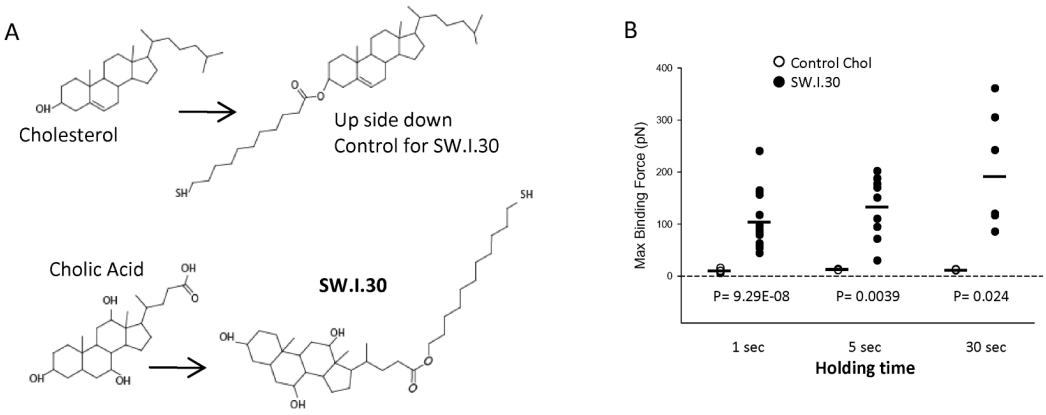

Fig 6. Synthetic cholesterol in its biological configuration shows directly binds to MSU surface

A. A schematic depiction of the substrates and end products for a modified cholesterol molecule (SW.I.30) suitable for binding to gold coated AFM cantilever in the orientation as in the plasma membrane, and its control in the reverse orientation. B. The binding forces between the AFM tip coated with SW.I.30 by SAM and the control. P values were calculated by the t-test on maximum adhesion forces. The black bar among the symbols is the average value for that group.

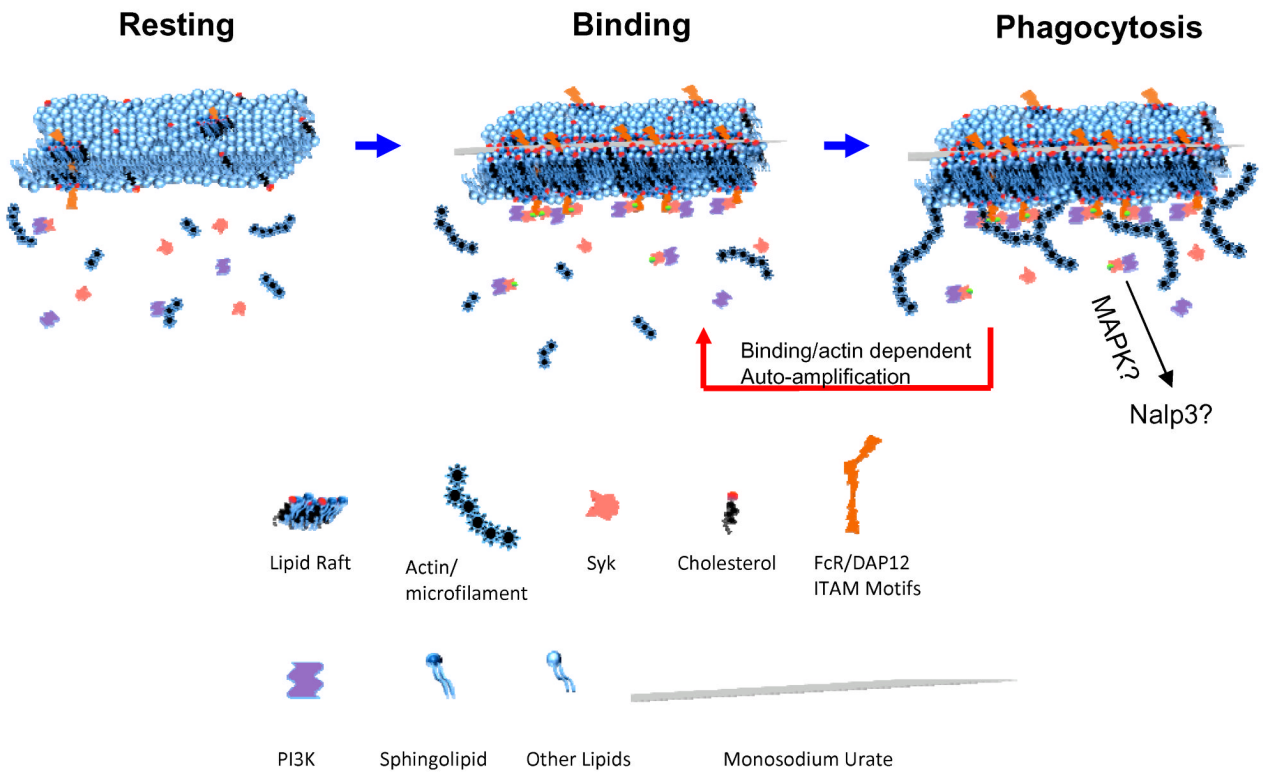

Fig 7. One possible/hypothetical scheme of the receptor independent Syk kinase activation

Left: Resting state DC membrane where lipid rafts are dispersed, and Syk recruitment to the inner membrane is limited. Middle: upon MSU binding, a lipid sorting event occurs as a consequence of potential interaction between the crystal surface and cholesterol (this point remains speculative). Such a sorting aggregates raft associated ITAM containing signaling molecules, leading to the recruitment of Syk, which in turn recruits PI3K. Right: Syk/PI3K leads to actin/microfilament and topological membrane changes that resemble phagocytosis, which further allows stronger and larger binding contacts in a manner of self-amplification. Since the binding strength increases without extracellular proteins (Fig. 3D), it remains unknown if the increased affinity is a result of more cholesterol binding or other lipid alterations that permit more intense membrane/solid surface interaction.